Ionics (2014) 20:875–886
DOI 10.1007/s11581-013-1026-7

ORIGINAL PAPER

Fabrication of highly selective PVA-g-GO/SPVA membranes via cross-linking method for direct methanol fuel cells

Myeongyeol Yoo · Myeongjin Kim · Yongseon Hwang · Jooheon Kim

Received: 16 August 2013 / Revised: 24 October 2013 / Accepted: 20 November 2013 / Published online: 27 December 2013

Abstract Organic/inorganic composite membranes were prepared using sulfonated poly(vinyl alcohol) (SPVA), mixed and cross-linked with different amounts of poly(vinyl alcohol)-grafted graphene oxide (PVA-g-GO). The introduction of PVA-g-GO to the membranes not only reduced the methanol permeability but also positively affected the mechanical properties: Increasing the PVA-g-GO content increased the blocking effect of GO. The PVA-g-GO/SPVA membranes were cross-linked with glutaraldehyde, resulting in the formation of cross-linking chains within the matrix, as well as between the matrix and the filler. Therefore, the microstructure of the PVA-g-GO/SPVA cross-linking membrane was different from that of the existing membranes. This structure also reduced the methanol permeability. The composite membranes exhibited proton conductivities ranging from 0.0141 to 0.0319 S/cm at 60 °C, and low methanol permeability ranging from 3.13×10^{-7} to 1.53×10^{-7} $cm^2\ s^{-1}$ at 25 °C.

Keywords Poly(vinyl alcohol) (PVA) · Graphene oxide · PVA-g-GO · Direct methanol fuel cell

Introduction

Direct methanol fuel cells (DMFCs) have received attention as a promising power source in fuel cell technology because of their stable operation, high energy efficiency, portability, and low environmental pollution [1, 2]. Polymer electrolyte membranes (PEMs), which transfer protons from the anode to the cathode and act as a barrier against fuel permeability, are vital components of DMFCs. Currently, perfluorosulfonic acid polymers such as Nafions are used as reference membranes for DMFCs because of their excellent chemical resistance and mechanical stability, as well as their high proton conductivity. However, Nafion has some specific limitations as well: high cost, methanol crossover, and loss of conductivity above 80 °C, which still restrict the performance and applications of DMFCs [3–5]. As alternatives to Nafion, many sulfonated polymers such as sulfonated poly(ether ether ketone), sulfonated poly(arylene ether sulfone), sulfonated poly(ether imide), and sulfonated polystyrene have been developed for fuel cell applications [6–10]. However, their proton conductivity is somewhat lower than that of Nafion because of their noncontinuous hydrophilic clusters.

Proton conductivity is crucial for improving the performance of DMFC membranes. A continuous hydrophilic cluster and the sulfonic acid group of the membranes are important for enhancing the proton conductivity. Poly(vinyl alcohol) (PVA) membranes have attracted attention because of their relatively low cost and high proton conductivity. They have natural hydrophilicity because of the many hydroxyl groups present in PVA, which is responsible for the high water uptake of the PVA membranes. Sulfonated PVA (SPVA) matrix, which has a sulfonic acid group, is used to enhance the Grotthuss mechanism. Consequently, the SPVA membranes have good proton conductivity values because of the high water uptake and high ion exchange capacity (IEC), which are needed for the vehicular mechanism and the Grotthuss mechanism, respectively. However, the SPVA membranes have high methanol permeability, which is attributed to the high water uptake. Moreover, they have poor mechanical and thermal properties for high water uptake [11–15].

In order to overcome the high methanol crossover and poor mechanical and thermal stabilities, two major approaches can be utilized. First, a filler can be introduced to the polymer matrix to improve the mechanical durability and to reduce the methanol permeability. Several fillers such as clay, silica,

M. Yoo · M. Kim · Y. Hwang · J. Kim (✉)
School of Chemical Engineering & Materials Science, Chung-Ang University, Seoul 156-756, Korea
e-mail: jooheonkim@cau.ac.kr

silicon-titanium oxides, and zirconium phosphate were introduced to the matrix to reduce the methanol permeability [16–19]. For example, Nafion 115 had lower methanol permeability when hydrophobic silica nanoparticle is introduced to the Nafion matrix [20], as well as when zirconium phosphate is introduced the matrix [21] compared to when they are introduced to a pure Nafion matrix. Wang et al. [22] reported zeolites on a chitosan/zeolite hybrid membrane that had a lower methanol permeability.

Recently, materials based on graphene oxide (GO) as fillers in polymer composites have attracted attention because of their potential for applications in nanocomposites and electronics. It has been reported that the improvement in the mechanical properties of polymers by adding graphene is much more efficient than by adding other nanofillers [23–27]. Moreover, GO has excellent thermal stability, high mechanical strength, a unique planar structure, and is electrically insulating. Ma et al. [27] reported the improved mechanical strength of epoxy/graphene nanocomposites. Luo et al. [28] synthesized graphene nanosheet/polystyrene nanocomposites and showed extraordinary low electrical percolation thresholds of 0.1 vol%. The PVA-grafted GO (PVA-g-GO) sheets were mixed with PVA in an aqueous solution to fabricate GO/PVA nanocomposites. Cheng et al. [29] showed the homogeneous dispersion of PVA-g-GO sheets in the PVA-g-GO/PVA nanocomposites. The PVA-g-GO/PVA nanocomposites were found to be much stronger and tougher than PVA. Moreover, the PVA-g-GO sheets were randomly dispersed throughout the composite films. The reinforcing mechanism of the PVA-g-GO/PVA composites is considered to be caused by the effective load transfer between the PVA matrix and the PVA-g-GO sheets via the strong interfacial adhesion between them.

The second approach involves mixing or cross-linking the membrane with hydrophobic materials in order to reduce the rate of water absorption because high rates of water absorption decrease the mechanical properties of the membranes. Many cross-linking matrices are already present in DMFC membranes [2, 30–32]. Zhong et al. [33] reported that the cross-linked sulfonated poly(ether ether ketone)/2-acrylamido-2-methyl-1-propanesulfonic acid blend membrane had low methanol permeability. Kim et al. [34] reported that PVA was cross-linked by sulfosuccinic acid (SSA), another cross-linking reagent, and that the methanol permeability value decreased with increasing SSA. In a previous cross-linking membrane study, only the matrix and the filler are mixed, and the matrix was cross-linked by a cross-linking agent or radiation. Therefore, the mechanical and thermal properties of the membranes were improved because of the characteristics of the filler and cross-linking with the matrix.

In this study, a novel PVA membrane is prepared using poly(vinyl alcohol)-grafted graphene oxide (PVA-g-GO) and SPVA. The effects of the cross-linked PVA-g-GO/SPVA composite membranes on the proton conductivity were examined. The SPVA matrix and PVA-g-GO were cross-linked with glutaraldehyde (GA) to determine its effect on a variety of membrane properties, including water uptake, mechanical and thermal durability, and methanol permeability.

Experiments

Materials

Graphite, with a mean particle size of <150 μm, was obtained from Sigma-Aldrich (Seoul, Korea). Potassium permanganate ($KMnO_4$), PVA, *N,N′*-dicyclohexylcarbodiimide (DCC), 4-dimethylaminopyridine (DMAP), dimethyl sulfoxide (DMSO), sodium hydride (NaH), Petroleum ether, Phenolpthalein (pH indicator), and sodium chloride (NaCl) were purchased from Sigma Chemicals (Seoul, Korea). Sulfuric acid (H_2SO_4), phosphoric acid (H_3PO_4), dimethylformamide (DMF), hydrochloric acid (HCl), hydrogen peroxide (H_2O_2), and acetone were purchased from Samchun Chemicals (Seoul, Korea). GA and propane sultone were purchased from TCI chemicals (Tokyo, Japan).

Synthesis of GO and PVA-g-GO

GO was synthesized using a modified Hummer's method [35]. The manufactured GO nanosheets were then functionalized with PVA by Steglich esterification (Scheme 1). Briefly, the purified GO (150 mg) was dissolved and sonicated in DMSO (45 mL) for 30 min to obtain a homogeneous brown solution. DCC (6.9 g, 33 mmol) and DMAP (0.51 g, 4.2 mmol) acted as catalysts in this reaction and were stirred together and then continuously added to the GO solution for 10 min. A solution of PVA in DMSO (100 mg/mL and 10 mL) was then added, and the resulting mixture was stirred at 50 °C for 3 days. When this process was completed, the resulting suspension was filtered through a 0.4-μm-thick nylon filter, and DMF and acetone were used to thoroughly wash the residue. To completely remove the unreacted PVA, the products were dissolved in hot water and filtered with a 0.4-μm-thick nylon membrane. Finally, the filtrates were washed with hot water and the PVA-functionalized GO was dried in a vacuum oven at room temperature. Scheme 1a gives a schematic diagram of PVA-g-GO esterification [29].

Synthesis of SPVA

SPVA was synthesized according to the following procedure (Scheme 1b). The mineral oil was removed from the NaH/mineral oil dispersion with petroleum ether. Pristine NaH and DMSO (150 mL) were added to a three-neck round bottom flask, flushed with nitrogen gas and allowed to react at 60 °C

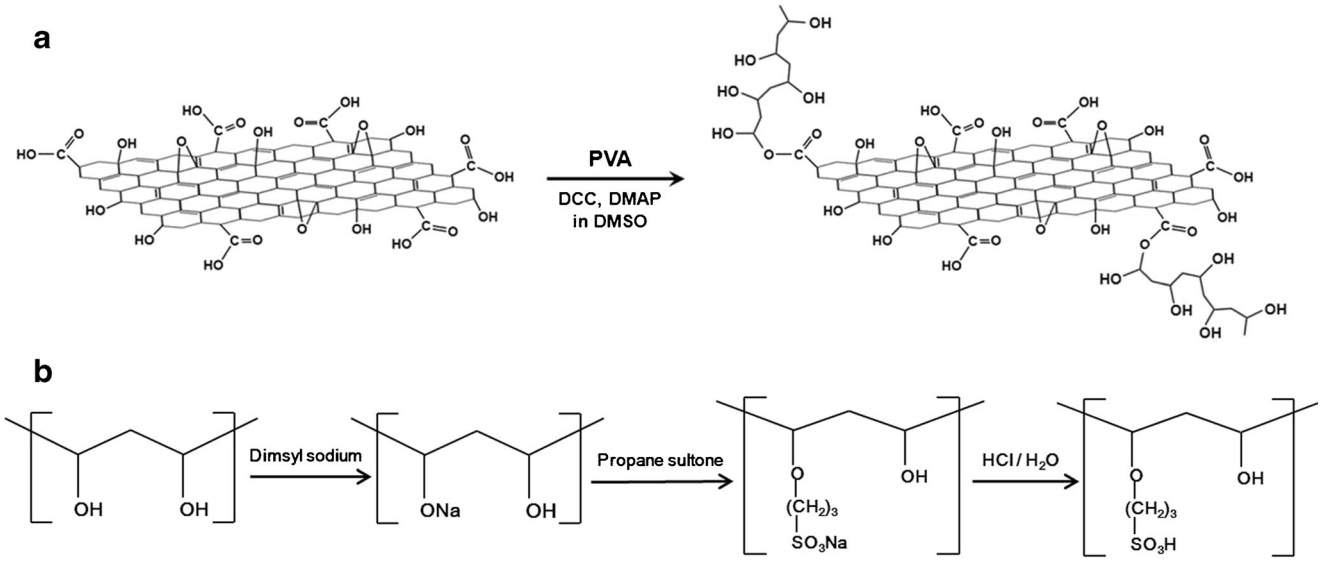

Scheme 1 **a** Poly(vinyl alcohol) (PVA)-grafted graphene oxide. **b** Sulfonated PVA matrix

for 3 h with mechanical stirring. Next, PVA (10 g) was added to the reaction mixture and stirred for 3 h. Propane sultone was then added dropwise to the mixture, after which the reaction mixture was stirred at 80 °C for 3 h. To replace the terminated Na with H, the PVA powder that had previously been reacted with the NaH/DMSO mixture was immersed into an HCl/water mixture for 12 h. The PVA was then filtered through a 400-nm-thick nylon membrane and washed several times with EtOH. The SPVA was dried for 4 h in a vacuum oven at 50 °C. Scheme 1b shows a schematic diagram of the sulfonation process of the PVA matrix.

Preparation of GO/PVA and PVA-g-GO/SPVA membranes and cross-linking treatment of PVA-g-GO/SPVA membrane

The GO was dispersed in water and the dispersed solution was blended with a PVA solution (water solution) at different

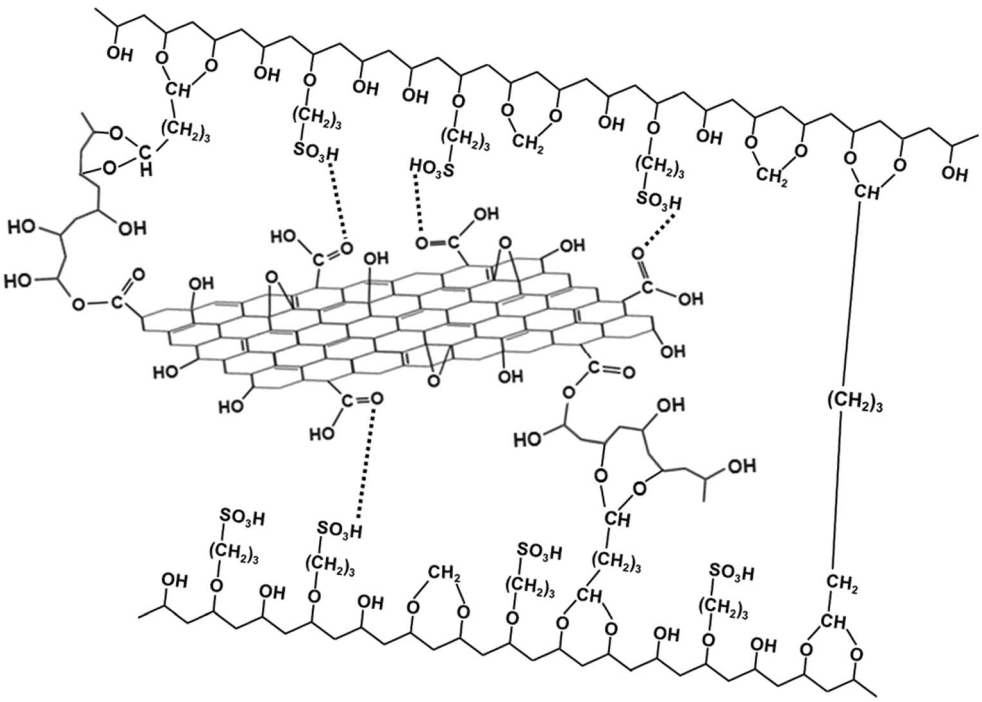

Scheme 2 Diagram of cross-linking between poly(vinyl alcohol)-grafted graphene oxide (PVA-g-GO) and sulfonated poly(vinyl alcohol) (SPVA)

ratios. The GO weight ratios of the blends were varied from 0 to 10 %.

The PVA-g-GO and GO were dispersed in water, and the resulting solutions were blended with SPVA and PVA solutions (water solutions) at different weight ratios. The PVA-g-GO and GO were dispersed over the range of 0–10 wt% of the matrix in deionized water. The dispersed mixtures were stirred and treated with ultrasonification. The PVA-g-GO and GO solutions were mixed with SPVA and PVA, respectively. The resulting PVA-g-GO/SPVA and GO/PVA solutions were poured into Petri dishes and dried at 40 °C for 24 h. After drying, the fabricated PVA-g-GO/SPVA and GO/PVA membranes were peeled off from the Petri dishes.

The thickness of the membranes was 100–110 μm. The cross-linking reaction was carried out by soaking the PVA-g-GO/SPVA membranes for 24 h at 40 °C in a cross-linking solution containing 5 wt% GA (50 wt% content in distilled water, TCI), HCl as an acid catalyst, and acetone. The resulting cross-linked membranes were washed with acetone and vacuum-dried at 40 °C for 24 h. Scheme 2 gives a schematic diagram of crosslinking between poly(vinyl alcohol)-grafted graphene oxide (PVA-g-GO) and sulfonated poly(vinyl alcohol) (SPVA).

Membrane characterization

Fourier transform infrared (FTIR) spectra of SPVA and PVA-g-GO were obtained using a Bio-rad FTS-1465 (USA). The IR spectra were collected over 32 scans in the 4,000–500 cm^{-1} region using the attenuated total reflectance mode at a resolution of 4 cm^{-1}. The microstructural transformation of the PVA-g-GO/SPVA composite membranes was analyzed using high-resolution field emission scanning electron microscopy (FE-SEM, Sigma. Carl Zeiss). The thermal degradation and stability of the membranes were investigated using a thermogravimetric analyzer (TGA, SCINCO TGA N-1000) at a heating rate of 10 °C/min from 30 to 800 °C. The differential scanning calorimetry (DSC, SETARAM instrument DSC 131evo) measurements were employed to study the thermal transition behavior of the membranes. The scans were conducted under nitrogen by heating the membranes to 250 °C with a heating rate of 10 °C/min. Dynamic mechanical analysis was performed using a Triton instrument. The samples were scanned from 25 to 110 °C at a heating rate of 5 °C/min.

Water uptake and swelling ratio

The s-PVA/PVA-g-GO membranes were vacuum-dried at 60 °C for 12 h, followed by weighing the dried membranes. The membranes were immersed in deionized water at different temperatures (25 and 60 °C). After 24 h, the surface solution on the wet membranes was removed with a tissue paper, and the wet membranes were then reweighed. The uptake was calculated using the following Eq. (1):

$$\text{Water uptake}(\%) = \frac{W_{\text{wet-dry}}}{W_{\text{dry}}} \times 100 \tag{1}$$

Ion exchange capacity

The IEC of the SPVA/PVA-g-GO membranes was measured by the titration method. Dry SPVA/PVA-g-GO membranes were immersed in a 1 mol solution of NaCl for 24 h to replace all the H^+ with Na^+. The amount of H^+ protons released from the membranes was determined by titration, using a 0.01 M NaOH solution with phenolphthalein as the pH indicator. The IEC value was obtained using the following Eq. (2):

$$\text{IEC} = \frac{\text{Consumed NaOH(mL)} \times \text{molality of NaOH}}{\text{Weight of dried membrane}} \left(\text{mequiv g}^{-1}\right) \tag{2}$$

Proton conductivity

The proton conductivity of the SPVA/PVA-g-GO membranes was measured using AC impedance spectroscopy (Zive-sp2, Zive-lab) between 0.1 kHz and 1 MHz. Before performing the conductivity experiments, all the samples were immersed in deionized water for at least 24 h at room temperature. The samples were then rapidly sandwiched between the two Pt electrodes. The proton conductivity of the GO/PVA and PVA-g-GO membranes was measured on a wet membrane. The conductivity of all the samples was measured using a two-point method at different temperatures (25 and 60 °C). The proton conductivity (σ) was calculated using the following Eq. (3):

$$\sigma = \frac{h}{(RS)} \tag{3}$$

where h is the thickness of the conducting membranes, R (Ω) is the electro-resistance, and S (m^2) is the surface dimension of the membranes.

Methanol permeability

The methanol permeabilities of the SPVA/PVA-g-GO membranes were measured using a glass diffusion cell composed of two reservoirs, each with a capacity of 100 mL. Before each test, the membranes were prehydrated. One reservoir was filled with a 10 M MeOH solution, and the second reservoir was filled with deionized water. Both compartments were stirred continuously with a magnetic stirrer during the permeability experiment. The methanol permeability was calculated using Eq. (4):

$$C_{\text{B}}(t) = \frac{A}{V_{\text{B}}} \frac{DK}{L} C_{\text{A}}(t - t_0) \tag{4}$$

where C_A and C_B are the concentrations of MeOH in the donor and receptor reservoirs, respectively. A and L are the diffusion area and thickness of the membrane, respectively. The product of D and K is the methanol permeability ($cm^2\ s^{-1}$).

Selectivity (determination of overall membrane characteristics)

Two membrane characteristics required for high performance in a DMFC are high proton conductivity and low methanol permeability. The membrane performance can be evaluated using the following expression (5):

$$\Phi = \frac{\sigma}{P} \tag{5}$$

where Φ is a parameter that evaluates the overall membrane performance in terms of the ratio of the ionic conductivity (σ) to the methanol permeability (P). Selectivity of the membrane for both proton conductivity and methanol permeability was calculated at 25 °C.

Result and discussion

Characterization of PVA-g-GO

The results of the FT-IR analysis indicated differences between the spectra of GO and PVA-grafted graphene oxide (PVA-g-GO). The spectra of both (a) pure GO and (b) PVA-g-GO are shown in Fig. 1. Both the broad peaks between 3,000 and 3,600 cm^{-1} are attributed to O–H stretching. The characteristic absorption bands for the methylene functional

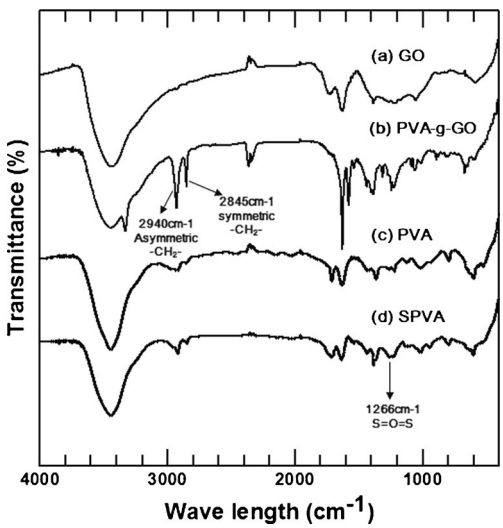

Fig. 1 Fourier transform infrared (FT-IR) spectra of graphene oxide and poly(vinyl alcohol)-grafted graphene oxide (PVA-g-GO)

group of PVA appeared at 2,940 cm^{-1} (–CH_2– asymmetric) and 2,845 cm^{-1} (–CH_2– symmetric), respectively. Moreover, a new peak appeared at 1,120 cm^{-1} (C–O–C stretch) representing the Steglich esterification effects of PVA-g-GO and SPVA. The formation of the new peaks indicated that the GO was functionalized by PVA.

The XPS spectra of GO, PVA-g-GO, PVA, and SPVA are shown in Fig. 2. The C 1s spectra of GO and PVA-g-GO are presented in Fig. 2c and e. A detailed analysis of the XPS spectra presented clear evidence that the GO was chemically modified, which was confirmed by the high-resolution spectra of C 1s and O1s based on a Gaussian spectral deconvolution. The C 1s peak of GO and PVA-g-GO appeared at 284.1, 286.1, and 288.0 eV. The C 1s specific peaks of GO and PVA-g-GO appearing at 284.1, 286.1, 288.0, and 288.6 eV, originated from the C–C, C–OH, C=O, and COOH functional groups. After the esterification reaction, the intensity of C–OH and C–C bonding increased with the addition of PVA. Moreover, a new peak appeared at 289 eV (COOR) on the C 1s peak from the PVA-g-GO sample. The O 1s peak appeared at 532.4 eV. The O 1s specific peaks of GO and PVA-g-GO are assigned to 531.2, 532.5, and 533.0 eV (Fig. 2d, f). After the reaction, the intensity of C–OH bonding slightly increased because of the increasing PVA content, and a new peak appeared at 534.4 eV (COOR), confirming the esterification. These results indicate that the PVA was successfully grafted on to the GO surface.

Figure 3 shows that the PVA-g-GO exhibit two distinct major degradation steps. The first step occurred at ~170 °C because of the loss of an oxygen-containing group from the GO. The second weight-loss step occurred from 250 to 350 °C and is assigned to the main-chain decomposition of PVA. The TGA was also used to measure the content of the PVA grafted on the GO. The weight loss of pristine GO at 600 °C was ~50 %, while that for PVA-g-GO was ~36 wt%. This result implies that the PVA-g-GO had ~25 wt% PVA and ~75 wt% GO and that 25 wt% PVA was grafted on the GO surface.

Characterization of SPVA

The effectiveness of the PVA sulfonation was examined using FTIR. Figure 1c and d shows the spectra of the pure PVA and SPVA membranes, respectively. Broad absorption bands were observed in both the pure PVA and SPVA membranes at 3,400 and 2,946 cm^{-1}, respectively. The former was assigned to the O–H stretching mode of the hydroxyl groups (–OH), and the latter to the asymmetric –CH_2– stretching band in the PVA matrix. Figure 1 shows the FTIR spectra of the SPVA membranes. Two new peaks appeared at ~1,266 cm^{-1}. The peak at 1,266 cm^{-1} was assigned to the asymmetric stretching vibrations of O=S=O in the sulfonic acid group.

The XPS spectra of the PVA show only two elements: C and O. However, the signal for S emerges in the spectra of

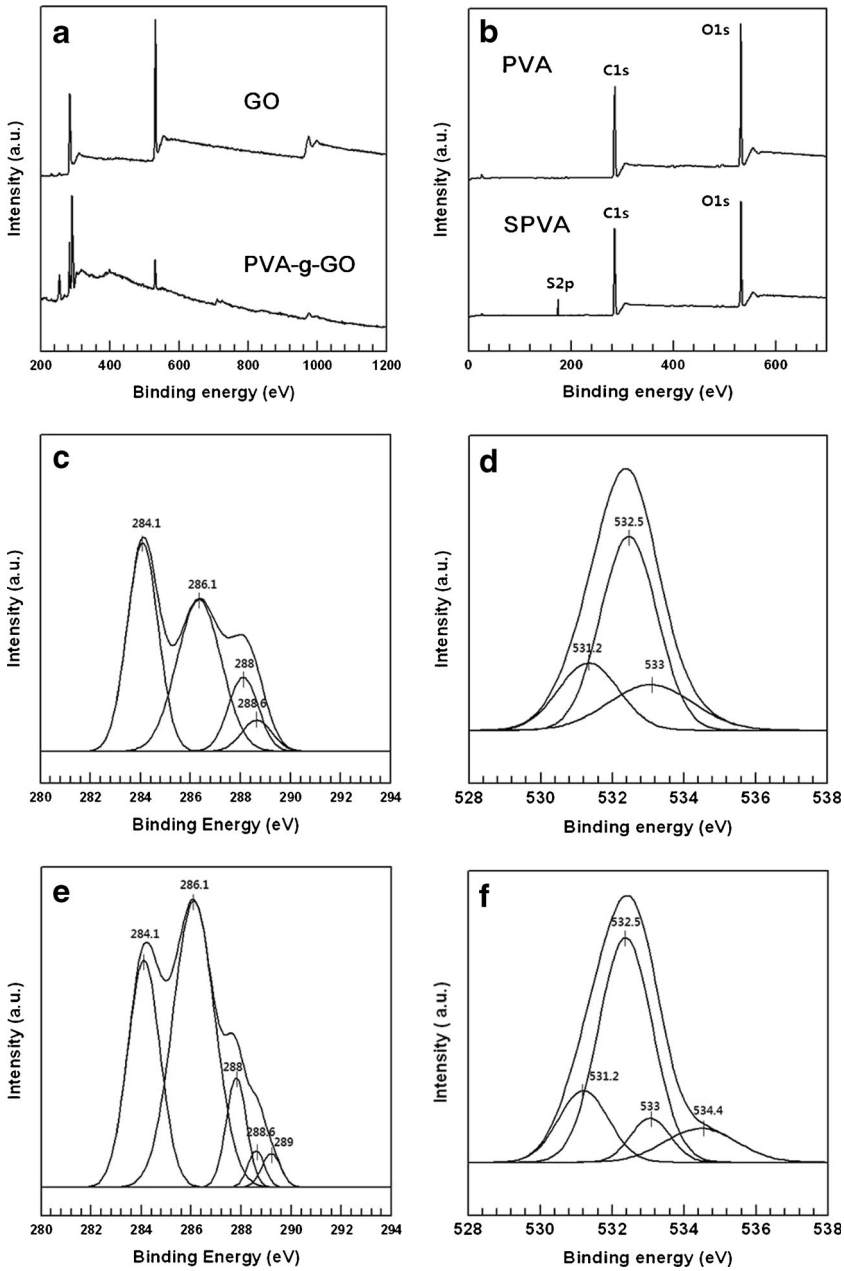

Fig. 2 Characterization results of graphene oxide (GO) and poly(vinyl alcohol)-grafted graphene oxide (PVA-g-GO): **a** wide scan of GO and PVA-g-GO; **b** wide scan of poly(vinyl alcohol) (PVA) and sulfonated poly(vinyl alcohol) (SPVA); **c** X-ray photoelectron spectroscopy (XPS) scan curve fitting of C 1s of GO; **d** O 1s of GO; **e** C 1s of PVA-g-GO; and **f** O 1s of PVA-g-GO. TGA curves of the pristine GO and the PVA-g-GO at a heating rate of 10 °C/min

SPVA. The C 1s and O 1s peaks are visible at 285 and 532 eV for the PVA and SPVA. Additionally, the S 2p peak is visible at 168 eV in the SPVA spectra. This indicates that the sulfur atom was successfully introduced on the PVA matrix by the reaction of the sulfonic acid groups with the hydroxyl groups of the PVA.

Characterization of PVA-g-GO/SPVA membrane

Figure 4a shows the microscale images of the cross-sectional areas of pristine PVA, Fig. 4b shows the image of the GO/PVA mixed membrane, and Fig. 4c and d shows the images of the cross-sectional area of the PVA-g-GO/SPVA (3 %) membrane. The different sizes of the GO and PVA-g-GO particles, which are uniformly distributed throughout the matrix, are visible in the PVA-g-GO/SPVA membrane images. The GO is present as micrometer-sized platelets, with a size of ~3–6 μm. The comparison of the GO/PVA and PVA-g-GO/SPVA membranes shows a difference in the filler dispersion in the matrix. In Fig. 4b, the GO particles of the GO/PVA membrane are partially agglomerated. In contrast, the PVA-g-GO particles of the PVA-g-GO/SPVA membrane are evenly dispersed in the SPVA membrane because of the compatibility between the PVA-g-GO and the SPVA. This difference is caused because the PVA-g-GO shows a greater dispersion in the SPVA membrane.

This phenomenon can be explained by hydrogen bonding between the sulfonating agent of SPVA and the functional

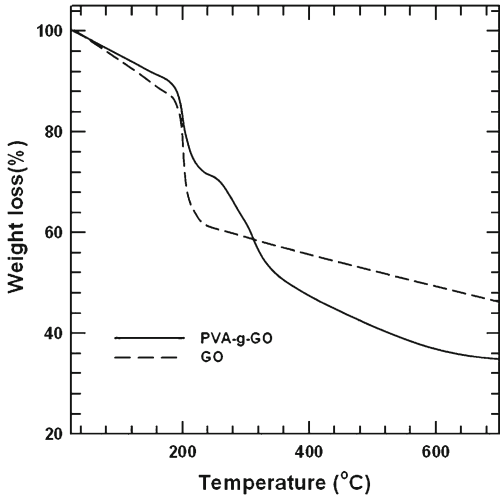

Fig. 3 Thermogravimetric analyzer (TGA) curves of pristine graphene oxide (GO) and poly(vinyl alcohol)-grafted graphene oxide (PVA-g-GO) at a heating rate of 10 °C/min

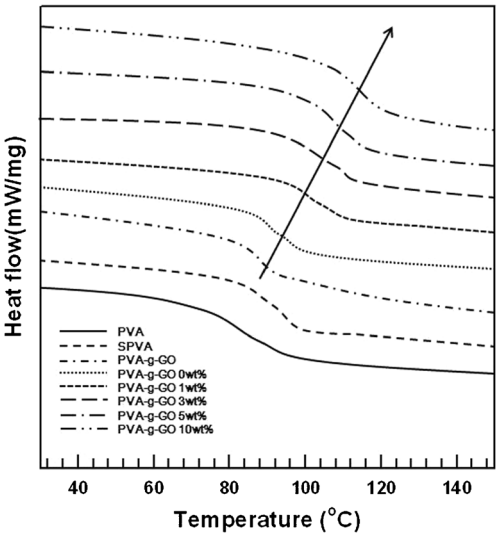

Fig. 5 Thermal analysis of differential scanning calorimetry (DSC) curve of poly(vinyl alcohol)-grafted graphene oxide/sulfonated poly(vinyl alcohol) (PVA-g-GO/SPVA) membranes

groups (CO, COOH) of GO in PVA-g-GO. Additionally, SPVA and PVA-g-GO have good compatibility because both have similar structures.

Thermal analysis of PVA-g-GO/SPVA membrane

Figure 5 shows the DSC curve for the SPVA membranes with different PVA-g-GO contents. The difference in the physical property of the SPVA membranes is reflected in the increase in the glass transition temperature (T_g). The T_g of the SPVA membrane (80 °C) was higher than that of the PVA membrane (74 °C) because the $–SO_3H$ group in the SPVA membrane formed hydrogen bonds that enhanced the strength of the polymer-chain interaction. T_g is strongly dependent on the mobility of the polymer chains. Viswanathan et al. reported that the T_g of polystyrene-grafted single-walled nanotubes (SWNTs) was higher than that of pure polystyrene and a polystyrene/SWNT mixture. The lower T_g can be attributed to the more mobile segments and the higher T_g to the segments with restricted mobility. In the PVA-g-GO membrane, PVA is part of the mobile segment and GO is part of the segment with restricted mobility. Therefore, the T_g of the PVA-g-GO (79 °C) is higher than that of PVA (74 °C). Meanwhile, the T_g of the PVA-g-GO/SPVA membrane increased with an increase in the PVA-g-GO content. This result is attributed to the increased cross-linking of SPVA with PVA on the PVA-g-GO.

The thermal stability and dimensional property of a PEM is a key factor for its durability during fuel cell operation at high temperatures [36]. The thermal stability of the SPVA

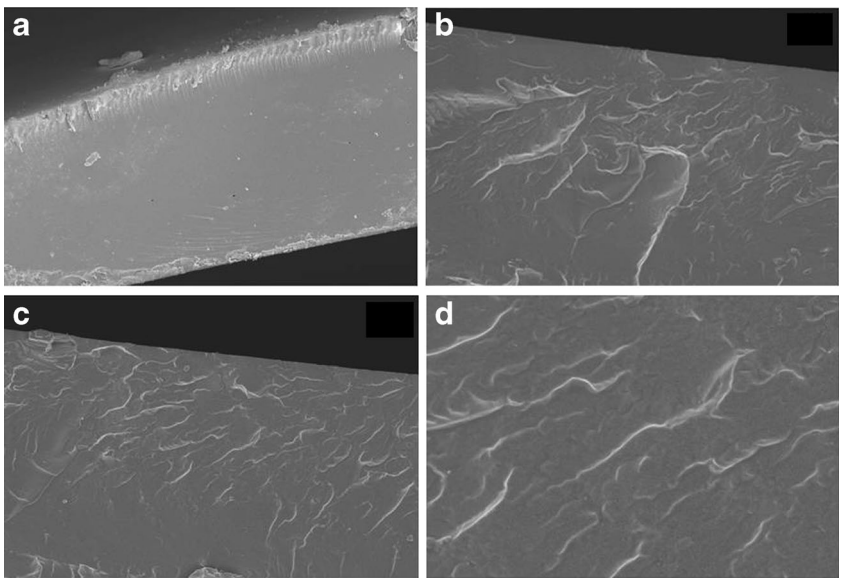

Fig. 4 Field emission scanning electron microscope (FE-SEM) images of **a** GO/SPVA, **b** GO/SPVA, **c** PVA-g-GO/SPVA, and **d** PVA-g-GO/SPVA. *GO/SPVA* Graphene oxide/sulfonated poly(vinyl alcohol); *PVA-g-GO/SPVA* poly(vinyl alcohol)-grafted graphene oxide/sulfonated poly(vinyl alcohol)

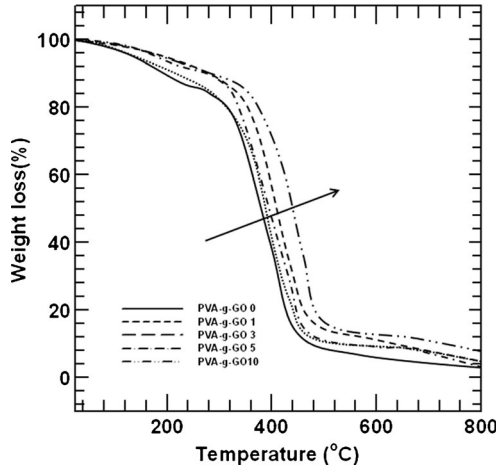

Fig. 6 Thermal analysis of thermogravimetric analyzer (TGA) curve of poly(vinyl alcohol)-grafted graphene oxide/sulfonated poly(vinyl alcohol) (PVA-g-GO/SPVA) membranes

membranes was examined using both TGA and DSC. Figure 6 shows the two steps of the TGA thermograph of the cross-linked PVA-g-GO/SPVA membrane with different PVA-g-GO contents. The first step occurs between 150 and 200 °C and is attributed to the decomposition of the hydroxyl groups of the PVA matrix. The second thermal degradation temperature was observed at ~300–480 °C because of the decomposition of the polymer main chain. On increasing the PVA-g-GO content, the thermal degradation temperature shifted to a higher temperature, indicating that the enhanced thermal stability is because of the increase in the degree of cross-linking, which can increase the resistance of the membranes to thermal degradation.

Water uptake and IEC

Water in proton exchange membranes is the major factor in proton conductivity because the absorbed water facilitates the transport of protons. That is, a higher water uptake facilitates the transport of protons, which significantly improves the fuel cell efficiency. However, excessive water absorption can degrade the mechanical stability of the membrane and aggravate the swelling problems, reducing the membrane performance. Therefore, it is very important to determine the water uptake of the membranes. The water uptake of the PVA-g-GO/SPVA membranes is high because hydrogen bonding with water molecules occurs between the hydroxyl (–OH) and sulfonic acid ($–SO_3H$) groups of SPVA and additional functional groups (–OH, C=O, –O–) of PVA-g-GO. Above 5 wt%, the PVA-g-GO component start to dominate, and the water uptake decreases because of the "blocking effect" of GO in PVA-g-GO, which is a barrier to water absorption. Moreover, the increased molecular interaction between the –OH and $–SO_3H$ groups in SPVA and the –O–, C=O, and –OH groups in PVA-g-GO also decreases the water uptake of the PVA-g-GO/SPVA membranes. Hydrophilic clusters, which have water-retention sites, also decrease because of the increased cross-linking that reduces the number of hydrophilic functional groups.

The IEC depends on the molar ratio of the sulfonic group in the polymer chain and the molar weight of the repeated unit. It is usually considered to correspond to the number of sites for proton transfer and has an important relationship with the proton conductivity. Therefore, the IEC of membranes is an important factor in determining the proton conductivity in DMFCs. The IEC of the GO/PVA membrane increased with increasing GO because protons are released from the carboxylic acid group of the GO. However, the IEC of the PVA-g-GO/SPVA membrane decreased with increasing PVA-g-GO because the sulfonic acid group releases more protons than the carboxylic acid group because of its strong acidity. Moreover, the carboxylic acid of GO reacted with the hydroxyl group of PVA, decreasing the proton-releasing group with increased PVA-g-GO contents in the PVA-g-GO/SPVA membranes. Based on these observations, it was concluded that the IEC value decreased with increasing PVA-g-GO.

Proton conductivity

A comparison of the water uptake and proton conductivity values provided in Tables 1 and 2 shows that the proton conductivity of PEMs depends on its water content. There are two mechanisms by which proton conduction can occur: the vehicular and Grotthus mechanisms. Both these mechanisms are strongly related to water uptake. In the vehicular mechanism, while diffusing through the aqueous media, water molecules act as the vehicles that carry protons along in forms such as H_3O^+, $H_5O_2^+$, and $H_9O_4^+$ [37]. The Grotthuss mechanism involves stationary water molecules where the protons hop from one water molecule to the next to transport protons along the hydrogen-bonded ionic channels. Consequently, when more water is present in the membrane, more hydrated species are generated, and therefore, more protons are transported. The SPVA membranes have high proton conductivity, in accordance with the sulfonic acid groups utilized in the Grotthuss mechanism. By comparing the proton conductivity of the PVA-g-GO/SPVA membrane with that of the GO/PVA membrane, it can be seen that the proton conductivity of the PVA-g-GO/SPVA membranes is higher than that of the GO/PVA membranes. The sulfonic acid group in the PVA-g-GO/SPVA membrane forms well-connected ionic channels, resulting in the enhanced transport of protons through the membrane. As shown in Table 1, with increasing content of the PVA-g-GO particles, the proton conductivity shows a decreasing trend at 5 % PVA-g-GO because of the blocking effect of GO. This means that the planar shape of GO in the PVA-g-GO/SPVA membrane effectively blocks the water-penetrating path and the movement of the polymer chain,

Table 1 Ion exchange capacity (IEC), water uptake, proton conductivity, and methanol permeability of poly(vinyl alcohol)-grafted graphene oxide/sulfonated poly(vinyl alcohol) (PVA-g-GO/SPVA) membranes

PVA-g-GO concentration (wt%)	IEC (mequiv g^{-1})	Water uptake (%)		Proton conductivity (S cm^{-1})		Methanol permeability (10^{-7} cm^2 s^{-1})
		25 °C	60 °C	25 °C	60 °C	
0	0.655	154.00	194.25	0.0206	0.0331	5.374
1	0.644	97.05	127.39	0.0197	0.0319	3.128
3	0.597	84.92	105.28	0.0189	0.0291	2.157
5	0.596	63.10	89.74	0.0143	0.0215	1.817
10	0.545	49.04	65.57	0.0097	0.0141	1.530

which enhanced the vehicular mechanism. Additionally, the ionic clusters in the membrane are also obstructed by the GO particles, which in turn is a barrier to water absorption that is required for the vehicular mechanism. The cross-linking reaction also reduces the proton conductivity because the cross-linking agent is hydrophobic, and therefore, the density of the hydroxyl group decreases, resulting in a decreased concentration of charge carriers in the membrane.

Methanol permeability

To fabricate DMFCs with high power density, a high concentration of methanol at low methanol permeability in aqueous solution should be used as fuel. Therefore, methanol permeability is important for DMFC applications. The methanol permeabilities of the cross-linked SPVA/PVA-g-GO membranes (0–10 wt%) ranged from 5.374×10^{-7} to 1.530×10^{-7} cm^2 s^{-1}, which were remarkably lower than Nafion® (2×10^{-6} cm^2 s^{-1}). The water and MeOH absorption of the SPVA membrane decreased on increasing the number of cross-linking sites. As shown in Table 1, when the number of the GO particles increases, the methanol permeability of the PVA-g-GO/SPVA membrane continuously decreases. Membranes with well-connected hydrophilic channels have high methanol permeability. However, because the dispersed GO particles in the GO/PVA and PVA-g-GO/SPVA membranes act as barriers to the connected hydrophilic channels, the GO particles obstruct the methanol from migrating through the membrane. Additionally, the interfacial interaction between the graphene-oxide-based materials (PVA-g-GO) and the SPVA polymer restricts the formation of the hydrophilic channels in the membrane, which also decreases the methanol permeability, because the methanol transport in these membranes requires relatively broad hydrophilic channels. The methanol permeability of the SPVA membrane (5.374×10^{-7} cm^2 s^{-1}) was higher than that of the PVA membrane (4.305×10^{-7} cm^2 s^{-1}) because methanol diffusion is enhanced by the $-SO_3H$ group, which exhibits a hydrophilic characteristic that promotes the vehicular mechanism of methanol transport. The PVA-g-GO/SPVA membranes show a dramatically decreasing tendency for methanol permeability on increasing the PVA-g-GO content when compared to the GO/PVA membranes because the PVA-g-GO particles are uniformly dispersed in the SPVA matrix owing to the compatibility between the PVA-g-GO and the SPVA. Moreover, the PVA-g-GO filler and the SPVA matrix are cross-linked in the PVA-g-GO/SPVA membranes. An increase in the degree of the cross-linking reaction decreases the concentration of the charge carriers in the membranes; therefore, the cross-linked membranes have lower methanol permeability than the mixed membranes. The cross-linking structure also restricts the mobility of the charged sites and decreases the free volume in these membranes, which may result in fewer and smaller hydrophilic pathways for carbonate mobility. Moreover, the PVA-g-GO/SPVA membrane was cross-linked between the matrix and the filler, which considerably decreased the free volume of the membrane and caused small hydrophilic pathways.

Selectivity

The PEMs in the DMFCs are required for obtaining high proton conductivity and low methanol permeability. The

Table 2 Ion exchange capacity (IEC), water uptake, proton conductivity, and methanol permeability of graphene oxide/poly(-vinyl alcohol) (GO/PVA) membranes

GO concentration (wt%)	IEC (mequiv g^{-1})	Water uptake (%)		Proton conductivity (S cm^{-1})		Methanol permeability (10^{-7} cm^2 s^{-1})
		25 °C	60 °C	25 °C	60 °C	
0	–	112.05	153.24	0.0178	0.0287	4.305
1	0.026	75.70	101.18	0.0159	0.0261	3.766
3	0.054	62.82	88.43	0.0141	0.0228	3.153
5	0.078	51.94	71.55	0.0103	0.0160	2.562
10	0.091	38.57	56.92	0.0062	0.0092	2.229

Table 3 Selectivity of poly (vinyl alcohol)-grafted graphene oxide/sulfonated poly(vinyl alcohol) (PVA-g-GO/SPVA) and Nafion membranes

PVA-g-GO concentration (wt%)	0	1	3	5	10	Nafion
Selectivity (S cm^{-3} s)	38,332.3	62,979.5	87,621.7	78,701.2	63,398.7	8,000

selectivity, which is defined as the ratio of proton conductivity to methanol permeability, is a factor for evaluating the membrane performance in terms of both proton conductivity and methanol permeability. The value of selectivity is usually used as an indicator for the applicability of membranes by comparing its value with those of commercial materials. A higher selectivity value infers better applicability in DMFCs. Table 3 shows the selectivity values of the PVA-g-GO/SPVA membranes and Nafion. The selectivity of the SPVA membrane was greatly enhanced with the introduction of PVA-g-GO, and PVA-g-GO/SPVA membranes showed better performance when compared to Nafion. These results are a direct result of the addition of PVA-g-GO and cross-linking in the membrane, which reduced the methanol permeability. The maximum selectivity value appears at 3 wt% of PVA-g-GO and is ~10 times that of the Nafion membrane. Therefore, the PVA-g-GO/SPVA membranes are promising materials for DMFC applications.

Mechanical durability

Figure 7 shows the mechanical properties of the SPVA membranes with different PVA-g-GO contents. Mechanical tests provide information on the durability of the PVA-g-GO/SPVA membranes. The addition of functionalized GO as the filler substantially influenced the mechanical properties of the PVA-g-GO/SPVA membranes. Figure 7a shows the substantially improved modulus of the PVA-g-GO/SPVA membranes compared to that of the SPVA membrane. Because graphene-based materials have an excellent elastic modulus (1,100 GPa) and intrinsic strength (125 GPa), the mechanical behavior of the PVA-g-GO/SPVA membranes was enhanced by increasing the PVA-g-GO content [38]. Another reason for the enhanced mechanical properties of the membranes is the interfacial adhesion of the functional groups between the PVA-g-GO and the SPVA. However, with further increase in the PVA-g-GO content from 5 to 10 wt%, the modulus only increased slightly from 2.9 to 3.1 GPa, which is ascribed to the phenomenon of restacking of the graphene-based material because of the van der Waals forces in the nanosheets. Slippage of the stacked graphene-based nanosheets will lead to less effective enhancement of the mechanical properties of the composites [25, 39]. Moreover, the cross-linking domains can help decrease the water uptake, which can in turn decrease the mobility of the polymer chains under stress. The tan delta curves of the PVA-g-GO/SPVA membranes as a function of temperature are shown in Fig. 7b. The value of the tan delta of the PVA-g-GO/SPVA membranes slightly decreased with increasing PVA-g-GO content, which is attributed to the obstruction of the motion of the matrix chains by the PVA-g-GO nanosheets.

Conclusion

The composite membranes of SPVA/PVA-g-GO with various compositions were prepared by a solution casting method. The PVA membranes, which are highly hydrophilic, originally exhibited good proton conductivity because of the vehicular mechanism that is responsible for high water uptake. The cross-linking chain formed not only between the matrices but also between the matrix and the filler with GA, resulting in a PVA-g-GO/SPVA cross-linked membrane with different microstructures compared to the existing membranes. The

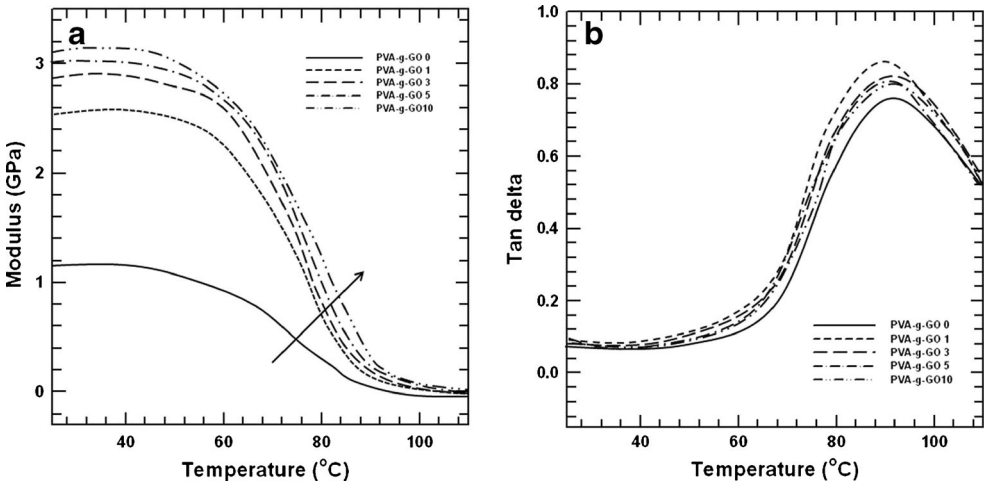

Fig. 7 **a** Storage modulus and **b** tan δ of poly(vinyl alcohol)-grafted graphene oxide/sulfonated poly(vinyl alcohol) (PVA-g-GO/SPVA) membranes

proton conductivity of the cross-linked PVA-g-GO/SPVA membrane slightly decreased the above effects. The GO in the membrane performed the role of the methanol barrier. Methanol permeability substantially decreased because of the GO barrier and cross-linking, especially the cross-linking between the matrix and the filler. Therefore, the PVA-g-GO/SPVA membranes have good selectivity because of the high proton conductivity and low methanol permeability. Moreover, GO provides good thermal and mechanical stability to the membranes. In addition, the PVA-g-GO dispersed well in the SPVA matrix because of the compatibility of their characteristics. Both the thermal and mechanical stability were enhanced by the cross-linking (PVA in PVA-g-GO and SPVA) and the characteristic of GO. Based on these results, it can be concluded that this membrane has good potential for use as PEMs in DMFC applications.

References

1. Shang Y, Xie X, Jin H, Guo J, Wang Y, Feng S et al (2006) Synthesis and characterization of novel sulfonated naphthalenic polyimides as proton conductive membrane for DMFC applications. Eur Polym J 42:2987–2993
2. Zhong S, Cui X, Cai H, Fu T, Zhao C, Na H (2007) Crosslinked sulfonated poly(ether ether ketone) proton exchange membranes for direct methanol fuel cell applications. J Power Sources 164:65–72
3. Zaidi SMJ, Mikhailenko SD, Robertson GP, Guiver MD, Kaliaguine S (2000) Proton conducting composite membranes from polyether ether ketone and heteropolyacids for fuel cell applications. J Membr Sci 173:17–34
4. Huang CH, Wu HM, Chen CC, Wang CW, Kuo P-L (2010) Preparation, characterization and methanol permeability of proton conducting membranes based on sulfonated ethylene-vinyl alcohol copolymer. J Membr Sci 353:1–9
5. Xue S, Yin G (2006) Proton exchange membranes based on poly(vinylidene fluoride) and sulfonated poly(ether ether ketone). Polymer 47:5044–5049
6. Gosalawit R, Chirachanchai S, Shishatskiy S, Nunes SP (2008) Sulfonated montmorillonite/sulfonated poly(ether ether ketone) (SMMT/SPEEK) nanocomposite membrane for direct methanol fuel cells (DMFCs). J Membr Sci 323:337–346
7. Jaafar J, Ismail AF, Matsuura T (2012) Effect of dispersion state of Cloisite15A® on the performance of SPEEK/Cloisite15A nanocomposite membrane for DMFC application. J Appl Polym Sci 124:969–977
8. Lee CH, Min KA, Park HB, Hong YT, Jung BO, Lee YM (2007) Sulfonated poly(arylene ether sulfone)–silica nanocomposite membrane for direct methanol fuel cell (DMFC). J Membr Sci 303:258–266
9. Yan J, Huang X, Moore HD, Wang C-Y, Hickner MA (2012) Transport properties and fuel cell performance of sulfonated poly(-imide) proton exchange membranes. Int J Hydrogen Energy 37: 6153–6160
10. Bae B, Kim D (2003) Sulfonated polystyrene grafted polypropylene composite electrolyte membranes for direct methanol fuel cells. J Membr Sci 220:75–87
11. Higa M, Sugita M, Maesowa S, Endo N (2010) Poly(vinyl alcohol)-based polymer electrolyte membranes for direct methanol fuel cells. Electrochim Acta 55:1445–1449
12. Qiao J, Hamaya T, Okada T (2005) New highly proton-conducting membrane poly(vinylpyrrolidone) (PVP) modified poly(vinyl alcohol)/2-acrylamido-2-methyl-1-propanesulfonic acid (PVA–PAMPS) for low temperature direct methanol fuel cells (DMFCs). Polymer 46: 10809–10816
13. Yang C-C, Lin C-T, Chiu S-J (2008) Preparation of the PVA/HAP composite polymer membrane for alkaline DMFC application. Desalination 233:137–146
14. Yang T (2009) Poly(vinyl alcohol)/sulfated β-cyclodextrin for direct methanol fuel cell applications. Int J Hydrogen Energy 34:6917–6924
15. Seeponkai N, Wootthikanokkhan J (2007) Proton conductivity and methanol permeability of sulfonated poly(vinyl alcohol) membranes modified by using sulfoacetic acid and poly(acrylic acid). J Appl Polym Sci 105:838–845
16. Kim TK, Kang M, Choi YS, Kim HK, Lee W, Chang H et al (2007) Preparation of Nafion-sulfonated clay nanocomposite membrane for direct menthol fuel cells via a film coating process. J Power Sources 165:1–8
17. Balbaşı M, Gözütok B (2010) Poly(vinyl alcohol)-colloidal silica composite membranes for fuel cells. Synth Met 160:150–155
18. Bauer F, Willert-Porada M (2005) Characterisation of zirconium and titanium phosphates and direct methanol fuel cell (DMFC) performance of functionally graded Nafion(R) composite membranes prepared out of them. J Power Sources 145:101–107
19. Raghuram V, gummaraju R, Moore RB, Mauritz KA (1996) Asymmetric Nafion/silicon oxide hybrid membranes via the *in situ* sol–gel reaction for tetraethoxysilane. J Polym Sci B Polym Phys 34: 2383–2392
20. Park CH, Kim HK, Lee CH, Park HB, Lee YM (2009) Nafion® nanocomposite membranes: effect of fluorosurfactants on hydrophobic silica nanoparticle dispersion and direct methanol fuel cell performance. J Power Sources 194:646–654
21. HOU H, SUN G, WU Z, JIN W, XIN Q (2008) Zirconium phosphate/Nafion115 composite membrane for high-concentration DMFC. Int J Hydrogen Energy 33:3402–3409
22. Wang J, Zheng X, Wu H, Zheng B, Jiang Z, Hao X et al (2008) Effect of zeolites on chitosan/zeolite hybrid membranes for direct methanol fuel cell. J Power Sources 178:9–19
23. Raza MA, Westwood A, Brown A, Hondow N, Stirling C (2011) Characterisation of graphite nanoplatelets and the physical properties of graphite nanoplatelet/silicone composites for thermal interface applications. Carbon 49:4269–4279
24. Teng CC, Ma CCM, Lu CH, Yang SY, Lee SH, Hsiao MC, Yen MY, Chiou KC, Lee TM (2011) Thermal conductivity and structure of non-covalent functionalized graphene/epoxy composites. Carbon 49: 5107–5116
25. Rafiee MA, Rafiee J, Wang Z, Song H, Yu ZZ, Koratkar N (2009) Enhanced mechanical properties of nanocomposites at low graphene content. ACS Nano 3:3884–3889
26. Medhekar NV, Ramasubramaniam A, Ruoff RS, Shenoy VB (2010) Hydrogen bond networks in graphene oxide composite paper: structure and mechanical properties. ACS NANO 4:2300–2306
27. Zaman I, Phan TT, Kuan HC, Meng Q, La LTB, Luong L, Youssf O, Ma J (2011) Epoxy/graphene platelets nanocomposites with two levels of interface strength. Polymer 52:1603–1611
28. Liu N, Luo F, Wu H, Liu Y, Zhang C, Chen J (2008) One-step ionic-liquid-assisted electrochemical synthesis of ionic-liquid-functionalized graphene sheets directly from graphite. Adv Funct Mater 18:1518–1525
29. Cheng HKF, Sahoo NG, Tan YP, Pan Y, Bao H, Li L et al (2012) Poly(vinyl alcohol) nanocomposites filled with poly(vinyl alcohol)-grafted graphene oxide. ACS Appl Mater Interfaces 4:2387–2394
30. Zhao C, Lin H, Na H (2010) Novel cross-linked sulfonated poly (arylene ether ketone) membranes for direct methanol fuel cell. Int J Hydrogen Energy 35:2176–2182

31. Luo H, Vaivars G, Mathe M (2009) Cross-linked PEEK-WC proton exchange membrane for fuel cell. Int J Hydrogen Energy 34:8616–8621
32. Zhang N, Zhang G, Xu D, Zhao C, Ma W, Li H et al (2011) Cross-linked membranes based on sulfonated poly (ether ether ketone) (SPEEK)/Nafion for direct methanol fuel cells (DMFCs). Int J Hydrogen Energy 36:11025–11033
33. Zhong S, Cui X, Cai H, Fu T, Shao K, Na H (2007) Crosslinked SPEEK/AMPS blend membranes with high proton conductivity and low methanol diffusion coefficient for DMFC applications. J Power Sources 168:154–161
34. KIM D (2004) Preparation and characterization of crosslinked PVA/SiO_2 hybrid membranes containing sulfonic acid groups for direct methanol fuel cell applications. J Membr Sci 240: 37–48
35. Hummers JWS, Offeman RE (1958) Preparation of graphitic oxide. J Am Chem Soc 80:1339
36. Tripathi BP, Shahi VK (2008) Functionalized organic-inorganic nanostructured N-p-carboxy benzyl chitosan-silica-PVA hybrid polyelectrolyte complex as proton exchange membrane for DMFC applications. J Phys Chem B 112:15678–15690
37. Mohtar SS, Ismail AF, Matsuura T (2011) Preparation and characterization of SPEEK/MMT-STA composite membrane for DMFC application. J Memb Sci 371:10–19
38. Zhao X, Zhang Q, Chen D, Lu P (2010) Enhanced mechanical properties of graphene-based poly(vinyl alcohol) composites. Macromolecules 43:2357–2363
39. Fang M, Wang K, Lu H, Yang Y, Nutt S (2009) Covalent polymer functionalization of graphene nanosheets and mechanical properties of composites. J Mater Chem 19:7098